Optimal Power Dispatching in the DC Microgrid with Clear Sky Irradiance Model

Hongwei Wu, Wenshuai Bai, Fabrice Locment, and Manuela Sechilariu

Abstract The optimization of power dispatching has been proved to be useful for reducing the operation energy cost of a microgrid based on photovoltaic source. However, the formulation of the optimization problem needs the weather forecast to predict photovoltaic generation. The current hourly forecast is always available and often lacks accuracy. Thus, this work proposes the optimization based on a clear sky model to predict the solar irradiance. This model has the advantage of simplicity, since it depends only on the geographical coordinates. The analyses have been done to compare the weather data during 5 months, and the validation of the proposed model is carried out by simulation. The results show the optimization results of the proposed model are slightly better than a common hourly forecast weather provided by a meteorological website.

1 Introduction

The DC microgrid has been the focus of research recently, because it can integrate effectively renewable resources, such as photovoltaic (PV) panels [1]. Particularly, the microgrid can be integrated into a building with rooftop PV panels to make a zero-energy or positive-energy building [2].

Similar to the traditional power grid, optimal power dispatching can reduce the power losses and the operation cost of the microgrid [3]. Till now, a lot of optimization algorithms have been developed, and among them, the mixed integer linear programming (MILP) method is widely used for being fast and effective [4, 5]. However, their effects depend highly on the accuracy of the load and production predictions [6]. For traditional grid, it involves only the load consumption prediction, which has been thoroughly studied [7] and can be adapted directly to the microgrid problems. However, in the context of microgrids based on

H. Wu (✉) · W. Bai · F. Locment · M. Sechilariu
Sorbonne University – Université de Technologie de Compiègne, Compiègne, France
e-mail: hongwei.wu@utc.fr; wenshuai.bai@utc.fr; fabrice.locment@utc.fr; manuela.sechilariu@utc.fr

W. Zamboni, G. Petrone (eds.), *ELECTRIMACS 2019*, Lecture Notes in Electrical Engineering 615, https://doi.org/10.1007/978-3-030-37161-6_38

renewable energy, the generation prediction is essential too [7]. Regarding the PV panels, the prediction concerns mainly on the solar irradiance for a given site [6]. Indeed, this is still a challenge. Even though the weather satellites can give precise information on a large scale, the high-resolution solar irradiance forecast is hardly accessible or costing at a high expense.

Large amount of precedent research concentrates on the local irradiance forecast problem. The solutions include using the numerical weather prediction model as stated in [8], analysing the satellite images [9] and using all-sky imager for cloud tracking [10]. Also, the statistical methods can be useful, such as the switching Markov model [11]. Recently, it is also popular to predict by the machine learning algorithms. In [12], the tree-based ensemble method predictions are presented and compared with a support vector regression predictor. In [13], the prediction is done by combining wrapper mutual information and extreme learning machine. Besides, the probabilistic forecast is another way to deal with the high variability of the renewable sources, such as presented in [14–16]. Unlike deterministic forecast, which outputs a series of fixed values, the probabilistic forecast produces most probable values with a certain interval. However, these methods need either the extra data, such as satellite images and all-sky image, or the long-term historical irradiance data to train the artificial intelligence model or establish the statistical model. Thus, the application is limited by the availability of these conditions.

This paper proposes to use the simple clear sky (CS) model to realize irradiance prediction. The advantage is that only the geographical coordinates of the site and the PV panel orientation are needed, which are accessible easily. The prediction results are compared with the real recorded data in Compiègne in Northern France, as well as the free accessible forecast data made by *Météo-France* (MF), during a period of 5 months in 2018. Moreover, the two sets of prediction are inputted into a MILP-based optimization solver to do the power dispatching, and the real data based simulations are done, in order to study the effectiveness of the prediction.

This paper is organized as follows: The clear sky model and MF forecast are presented and compared in Sect. 2, and the optimization problem of a DC microgrid is given in Sect. 3, followed by the simulation and the results presented in Sect. 4. The final conclusion is given in Sect. 5.

2 Weather Forecast

In the context of microgrid power dispatching, the weather forecast is often expected to give the solar irradiance prediction for the day-ahead and intraday optimization. Thus, the prediction time horizon should cover the whole PV operation period. In this paper, the daily period is set from 9:00 to 18:00.

2.1 Clear Sky Irradiance Model

The CS model is a method based on geometric calculation to predict solar irradiance on a specific surface while no cloud influence is considered. Obviously, it is accurate only in sunny days, but its accuracy is acceptable when the sky is not heavily covered. This is particularly useful for PV panels, since they are mostly installed in sunny regions.

Since the CS model is classical, one common method is adopted in this work, and more details can be found in [17].

The beam radiation on earth g_b can be simply expressed as follows:

$$g_b = g_{sc} \cdot T^m. \tag{1}$$

g_{sc} is the extraterrestrial solar irradiation and can be set as 1367 W/m^2. T is the atmospheric transmittance for short wave solar irradiance and can be seen as 0.7 for simplicity. m is the air mass coefficient, and it is approximately expressed by the local zenith angle θ_z as given in Eq. (2):

$$m = \frac{1}{\cos(\theta_z)}. \tag{2}$$

The beam radiation on a given sloped surface can be then determined as the following:

$$g_{bg} = g_b \cdot \cos\theta. \tag{3}$$

θ is the angle of incidence between the beam irradiance on the surface and the normal to the surface. An approximate expression of θ is given in Eq. (4).

$$\begin{aligned} \cos\theta = {} & \sin\delta \cdot \sin\varphi \cdot \cos\beta - \\ & \sin\delta \cdot \cos\varphi \cdot \cos\beta \cdot \cos\gamma \\ & + \cos\delta \cdot \cos\varphi \cdot \cos\beta \cdot \cos\omega \\ & + \cos\delta \cdot \sin\varphi \cdot \sin\beta \cdot \cos\gamma \cdot \cos\omega \\ & + \cos\delta \cdot \sin\varphi \cdot \sin\gamma \cdot \sin\omega \end{aligned} \tag{4}$$

where δ is the declination angle of the sun at the solar noon, φ is the latitude, β is the slope angle of the given surface, γ is the surface azimuth angle which is 0 if due south and ω is the hour angle. It is evident that these data can be derived from the geographical coordinates and the slope of the given surface, i.e. the installed PV panels. All of them are easily accessible for any PV installation.

Besides, the diffuse radiation on the surface g_{dg} is obtained by Eq. (5).

$$g_{dg} = 0.3 \cdot \left(1 - T^m\right) \cdot \frac{(1 + \cos\beta)\, g_{sc}}{2} \cdot \cos\theta. \tag{5}$$

The reflect radiation may exist if there exists any building near the PV panels. However, it needs a complex geometric modelling and differs from one site to another. Thus, it is not considered in this work. As a result, the total radiation g_{tg} obtained by the clear sky model is the sum of the beam radiation and the diffuse radiation.

$$g_{tg} = g_{bg} + g_{dg}. \tag{6}$$

2.2 *Météo-France Forecast*

MF is a public establishment that offers meteorological information in France. It offers high-resolution metrological forecast covering all the French territory under open licence [18]. The forecast is generated by the AROME model, and the geographical resolution is 0.025°, which corresponds to an area of 6.25 km^2. The hourly forecast is made several times per day including the accumulated ground solar radiation in J/m^2. Aiming at the day-ahead optimization, this work focuses on the forecast made at midnight. In order to obtain the instant solar irradiance, a hypothesis is made assuming that the irradiance is homogeneous in the area and uniformly distributed in the 1-h interval.

2.3 *Case Study*

A group of PV panels are installed in the parking area of Université de Technologie de Compiègne as depicted in Fig. 1, whose coordinates are 49.401°N, 2.796°E. The PV panels are with a slope of 4° and an azimuth angle of −97°, almost in the direction of east. In addition, a sensor system is installed to record the instant solar irradiance on the panels at every 10 s.

In order to validate the CS model, the instant irradiance prediction given by CS model is compared with the recorded data for sunny days as depicted in Fig. 2. The blue and red curves are the beam radiation and total radiation obtained by the CS model, and the yellow curve is the recorded real data.

In Fig. 2a, the real irradiance is close to the beam radiation except for the early hours in the morning. On the contrary, the real irradiance is close to the total radiation in Fig. 2b. This is because the buildings nearby are sheltering the PV panels from the diffuse radiation, when the sun position is high. This is the case of Fig. 2a. When the sun position is relatively low, the same buildings reflect the solar irradiance on the PV panels.

Since the hourly forecast from MF is of ladder form and the visual comparison to the continuous curve in Fig. 2 is not significant, the hourly average irradiances are compared in Fig. 3, in which the yellow bar represents the MF forecast. It can be seen that this forecast gives a higher prediction than the total radiation from

Fig. 1 Photovoltaic panels in the campus in Compiègne, France

the CS model but close to the real irradiance on the 26th June 2018. However, the forecast on the 10 October is far from the reality. The real irradiance of this day is even higher than the total radiation of the CS model, meaning the atmospheric transparency T is exceptionally higher than 0.7. Besides the graphs, some usual statistical indicators can help to compare the CS prediction and the MF forecast with the recorded data, such as mean absolute error (MAE), mean bias error (MBE), root mean square error (RMSE), mean absolute percentage error (MAPE) and Pearson correlation coefficient (ρ). They are defined as follows:

$$\mathrm{MAE} = \frac{1}{n}\sum_{k=1}^{n}\left|g_{\mathrm{pred,k}} - g_{\mathrm{real},k}\right|. \tag{7}$$

$$\mathrm{MBE} = \frac{1}{n}\sum_{k=1}^{n}\left(g_{\mathrm{pred,k}} - g_{\mathrm{real},k}\right). \tag{8}$$

$$\mathrm{RMSE} = \sqrt{\frac{1}{n}\sum_{k=1}^{n}\left(g_{\mathrm{pred},k} - g_{\mathrm{real},k}\right)^2}. \tag{9}$$

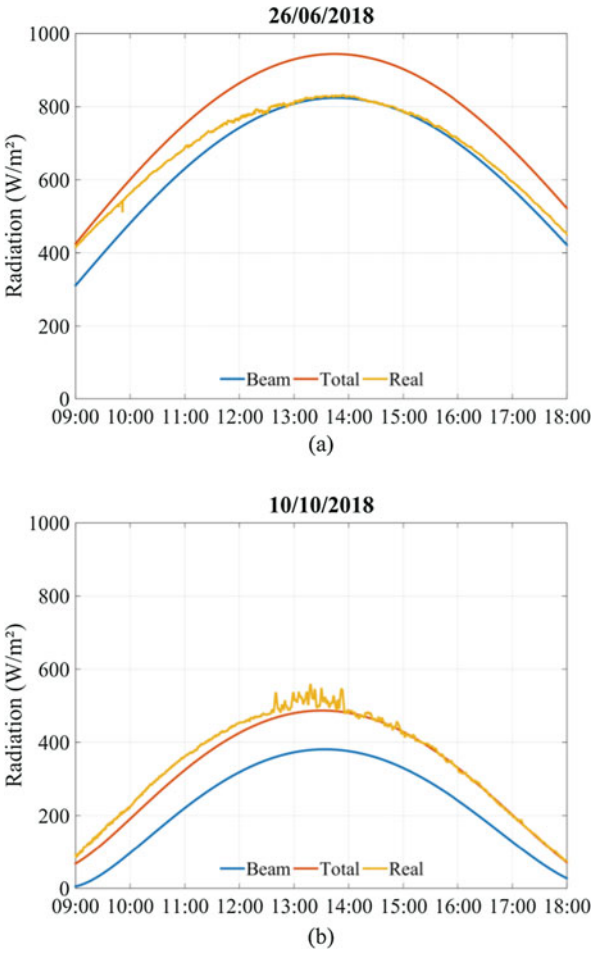

Fig. 2 Instant irradiance comparison between the prediction given by CS model and recorded data: (**a**) on the 26th June 2018; (**b**) on the tenth October 2018

$$\mathrm{MAPE} = \frac{1}{n}\sum_{k=1}^{n}\left|\frac{g_{\mathrm{pred},k} - g_{\mathrm{real},k}}{g_{\mathrm{real}k}}\right| \cdot 100\%. \tag{10}$$

$$\rho = \frac{\mathrm{cov}\left(g_{\mathrm{pred}}, g_{\mathrm{real}}\right)}{\sigma_{\mathrm{g}}\mathrm{pred} \cdot \sigma_{\mathrm{g}}\mathrm{real}}. \tag{11}$$

$g_{\mathrm{pred},k}$ is kth predicted irradiance and $g_{\mathrm{real},k}$ is kth real irradiance. $\mathrm{cov}(g_{\mathrm{pred}}, g_{\mathrm{real}})$ indicates the covariance between the prediction and the reality; $\sigma_{\mathrm{g\_pred}}$ and $\sigma_{\mathrm{g\_real}}$ are the standard deviation of the predicted irradiance and that of the real irradiance, respectively.

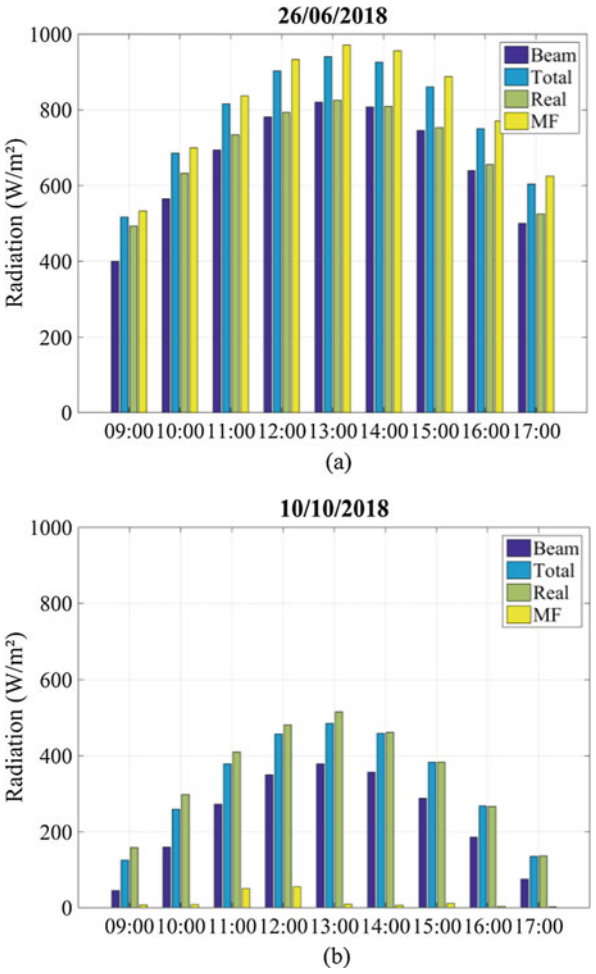

Fig. 3 Hourly average irradiance of the predictions and the recorded data: (a) on the 26th June 2018; (b) on the tenth October 2018

MAE and MBE tell the mean accuracy of the prediction without and with the bias. A positive bias means the over-prediction, whereas negative means the under-prediction. RMSE value is more impacted by the large errors than by the small ones. MAPE reflects the average relative error. ρ describes the linear similarity between the prediction and the reality. From Table 1, it can be seen that the CS prediction is superior to the MF forecast, since the values of MAE, MBE, RMSE and MAPE are smaller, meaning less error, and the Pearson coefficient is higher. It validates the CS model in case of sunny days.

Further validation must be done for longer period. The studied site is located in Northern France, and in winter day, little PV generation can be made. Thus, a 5-month study, dated from the third June to the 31st October 2018, is carried out (except the eighth October, data unavailable due to system maintenance). The

Table 1 Statistical comparison of 2 sunny days

Statistics	26th June 2018		10th October 2018	
	Clear sky	MF	Clear sky	MF
MAE	86.69	110.02	18.96	329.00
MBE	86.69	110.02	−17.75	−329.00
RMSE	91.85	115.48	24.86	350.97
MAPE	10.80%	15.59%	7.49%	95.64%
ρ	99.39%	99.26%	99.16%	48.28%

Table 2 Statistical comparison for 5 months

Statistics	Clear sky	MF
Average MAE	197.35	208.60
Average MBE	184.62	141.22
Maximal RMSE	627.44	549.56
Average MAPE	33.69%	97.85%
Average ρ	62.32%	62.75%

statistics are done each day between 9:00 and 18:00, and the results are given in Table 2.

The mean MAE of the CS model is close to the mean MBE, since in cloudy days the model always tends to over-predict. On the contrary, the average MBE for MF forecast is obviously less, since it can both over- and under-predict the irradiance. The maximal RMSE of CS model is quite large, and it is surely due to the bad weather, such as the heavy rain. But the MAPE of 33% is acceptable for such a simple model, especially when compared to the nearly 100% of MF forecast. In the end, both predictions present a Pearson coefficient of 62%, meaning in general the predictions are synchronized with the reality.

3 Prediction in the Optimization Problem for DC Microgrid Power Dispatching

The power dispatching problem in this work is formulated according to a building-integrated microgrid as depicted in Fig. 4. It is composed of a group of PV panels, an energy storage system, a connection to the public grid and the loads in the building. All these components are connected to a common capacitive DC bus via power converters. The PV panels are driven by a maximal power point tracking (MPPT) algorithm in most of time, but it is possible to shed some PV power $p_{\mathrm{PV\_S}}$ to limit the power injected into the bus p_{PV} if needed. The energy storage system is classical lead acid batteries and can be discharged or charged with the power $p_{\mathrm{S\_D}}$ or $p_{\mathrm{S\_C}}$ to supply the load or absorb the excessive PV generation. Similarly, the grid can supply power to the microgrid with the power $p_{\mathrm{G\_S}}$ as well as absorb the power $p_{\mathrm{G\_I}}$ from the microgrid. The loads in the building are seen as a single power demand

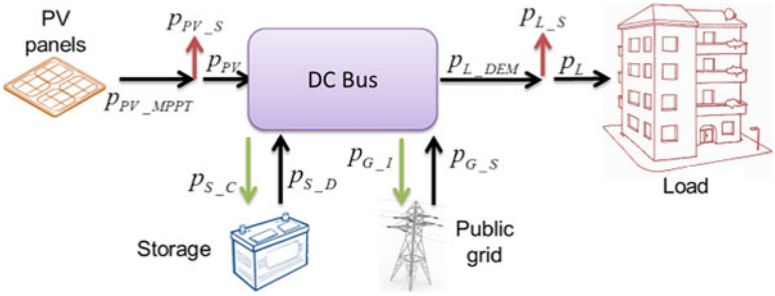

Fig. 4 Topology of the studied DC microgrid

$P_{\mathrm{L\_DEM}}$. If the available power is insufficient, the real load power P_{L} can be shed to keep the power balance.

Some constraints, physical and regulatory, must be respected in the microgrid operation. For example, the state of charge (SOC) of the storage, as defined in Eq. (12), must be kept in a certain range to avoid over-discharge and overcharge. In Eq. (12), v_{S} is the storage voltage and C_{REF} is the battery capacity in Ah, while SOC_0 is the initial value.

$$\mathrm{soc}\left(t_i\right) = \mathrm{SOC}_0 + \frac{\sum_{t=t_0}^{t_i} \left[p_{\mathrm{S}}\mathrm{C}\left(t_i\right) - p_{\mathrm{S}}\mathrm{D}\left(t_i\right)\right] \Delta t}{3600 \cdot v_{\mathrm{S}} \cdot C_{\mathrm{REF}}}. \tag{12}$$

The power supplied or absorbed by the storage and the grid must be constrained owing to the component capacity. Furthermore, the microgrid is neither allowed to charge the battery by the grid power nor inject the power into the grid while discharging the battery.

The goal of the optimal power dispatching is to maximize the PV generation and respond to the load power demand. In this objective, the operation energy cost for each element is defined in Eq. (13):

$$\begin{aligned} C_{\mathrm{PV}}\mathrm{S} &= \sum_{t_i=t_0}^{t_F} T_{\mathrm{PVS}} \cdot \Delta t \cdot p_{\mathrm{PV}}\mathrm{S}\left(t_i\right) \\ C_{\mathrm{S}} &= \sum_{t_i=t_0}^{t_F} T_{\mathrm{S}} \cdot \Delta t \cdot \left[p_{\mathrm{S}}\mathrm{C}\left(t_i\right) + p_{\mathrm{S}}\mathrm{D}\left(t_i\right)\right] \\ C_{\mathrm{G}} &= \sum_{t_i=t_0}^{t_F} T_{\mathrm{G}} \cdot \Delta t \cdot \left[p_{\mathrm{G}}\mathrm{S}\left(t_i\right) - p_{\mathrm{G}}\mathrm{I}\left(t_i\right)\right] \\ C_{\mathrm{L}}\mathrm{S} &= \sum_{t_i=t_0}^{t_F} T_{\mathrm{LS}} \cdot \Delta t \cdot p_{\mathrm{L}}\mathrm{S}\left(t_i\right) \end{aligned} \tag{13}$$

Based on the above definitions and constraints, the power dispatching optimization problem can be formulated as following:

$$
\begin{aligned}
&\text{Minimize } C_{\text{TOTAL}} = C_{\text{G}} + C_{\text{S}} + C_{\text{PVS}} + C_{\text{LS}} \\
&\text{with respect to} \\
&p_{\text{PV}}(t_i) + p_{\text{GS}}(t_i) + p_{\text{SD}}(t_i) = p_{\text{L}}(t_i) + p_{\text{SC}}(t_i) + p_{\text{GI}}(t_i) \\
&\text{SOC}_{\text{MIN}} \le \text{soc}(t_i) \le \text{SOC}_{\text{MAX}} \\
&0 \le p_{\text{PVS}}(t_i) \le p_{\text{PV MPPT}}(t_i) \\
&0 \le p_{\text{SD}}(t_i) \le P_{\text{S MAX}}, \quad 0 \le p_{\text{SC}}(t_i) \le P_{\text{S MAX}} \\
&0 \le p_{\text{GI}}(t_i) \le P_{\text{GI MAX}}, 0 \le p_{\text{GS}}(t_i) \le P_{\text{GS MAX}} \\
&\text{if } p_{\text{PV}}(t_i) - p_{\text{L}}(t_i) \ge 0, \text{then } p_{\text{SD}} = 0, p_{\text{GS}} = 0 \\
&\text{else}, \quad p_{\text{SC}} = 0, p_{\text{GI}} = 0
\end{aligned}
\tag{14}
$$

MILP solver is suitable for this problem, but the accurate PV generation prediction is essential. For a given PV panel, its generation depends mostly on the solar irradiance. If the predicted irradiance is not accurate enough, the optimization results can be invalidated. Thus, the accuracy of the irradiance prediction has a direct impact on the operation energy cost of the microgrid.

4 Simulation Validation

In order to test the CS prediction in the realistic scenarios, the simulation of the microgrid is realized with the 5-month data. The simulation includes a two-layer structure. The upper layer inputs the predictions into IBM CPLEX optimization solver and outputs the power dispatching reference. The lower layer, consisting of a MATLAB/Simulink model of the microgrid, computes the real operation cost while taking the recorded irradiance data and the power dispatching reference into account. The values of the parameters are given in Table 3.

Aiming at simplifying the comparison, a same load profile is used in the optimization and simulation for all the 150 days. The optimization is operated twice for each day, using, respectively, the CS prediction and the MF forecast. A typical profile is shown in Fig. 5, in which the difference between the prediction and the real production can be seen.

As a result, the CS prediction has a total cost of 12.4 € for the 150 days, and the MF forecast has 14.7€. For a more detailed analysis, a daily relative cost difference Δ is defined as in Eq. (15)

Table 3 Microgrid parameters

Parameters	Values	Parameters	Values
PV peak power	4140 Wc	T_{PVS}	0.7 €/kWh
Storage capacity	185 Ah	T_{LS}	1.5 €/kWh
Storage voltage	96 V	T_{S}	0.01 €/kWh
Storage power limit	±3000 W	T_{G}	0.1 €/kWh
Grid power limit	±3000 W	SOC limit	[20%, 80%]

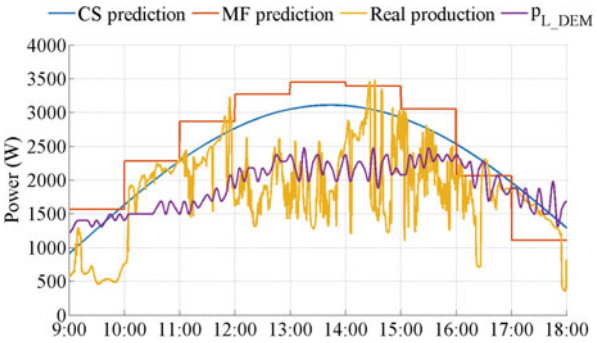

Fig. 5 PV generation and load profiles on the 31st August 2018

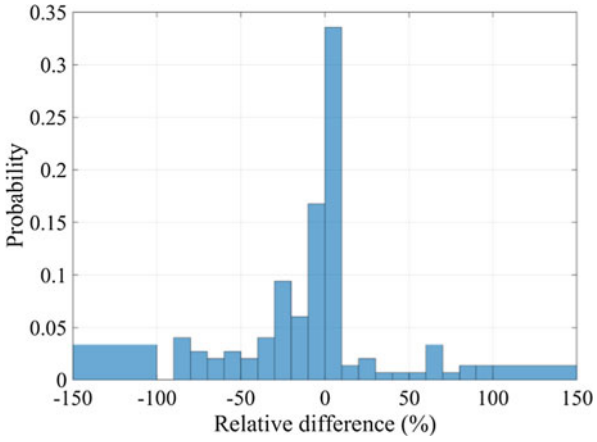

Fig. 6 Distribution of relative difference of the operation cost

$$\Delta = \frac{C_{\mathrm{CS}} - C_{\mathrm{MF}}}{|C_{\mathrm{MF}}|} \cdot 100\%. \tag{15}$$

C_{CS} and C_{MF} are, respectively, the daily cost based on CS prediction and on MF forecast. Hence, Δ is positive if the CS prediction leads to a higher cost. The distribution of Δ during the 150 tested days is shown in Fig. 6. It can be figured out that the relative difference is mostly in the range of 0–10%, meaning in most days the operation cost for CS prediction is slightly higher than that of MF forecast. Though, the probability of Δ being negative is higher than that of being positive. That explains why the total cost of CS prediction is lower than the other.

The results show that the open licence MF forecast is not accurate enough for the microgrid power dispatching, since the geographical resolution is not high enough and the hourly forecast cannot cover the high variability of the solar irradiance. Hence, the CS prediction can be useful for sites for which more precise forecast is unavailable.

5 Conclusions

The power dispatching of a PV-based microgrid can help in improving the performance, but the prediction of the solar irradiance is necessary. In this paper, a CS model is presented to predict the solar irradiance on the PV panels. This model involves only geometric calculation and thus can be widely applied and requires no extra instrument or historical data. A case study is carried out to compare the CS prediction with the free available MF forecast during 5 successive months in 2018. Moreover, the optimal power dispatching is done with the same data. The simulation results show that the proposed model can lead to less operation cost than the MF forecast, even though some prediction errors persist. In conclusion, the clear sky irradiance model can play a key role for low-cost optimal power dispatching.

References

1. M. Sechilariu, F. Locment, D.C. Urban, *Microgrid: Intelligent Control and Power Flow Optimization* (Elsevier, Amsterdam, 2016). ISBN: 978-012803736-2
2. E. Rodriguez-Diaz, J.C. Vasquez, J.M. Guerrero, Intelligent DC homes in future sustainable energy systems: when efficiency and intelligence work together. IEEE Consum. Electron Mag. **5**(1), 74–80 (2016)
3. A. Anvari-Moghaddam, J.M. Guerrero, J.C. Vasquez, H. Monsef, A. Rahimi-Kian, Efficient energy management for a grid-tied residential microgrid. IET Gener. Transm. Distrib. **11**(11), 2752–2761 (2017)
4. L. Bartolucci, S. Cordiner, V. Mulone, V. Rocco, J.L. Rossi, Renewable source penetration and microgrids: Effects of MILP-based control strategies. Energy **152**, 416–426 (2018)
5. M. Sechilariu, B.C. Wang, F. Locment, Supervision control for optimal energy cost management in DC microgrid: design and simulation. Int. J. Electr. Power Energy Syst. **58**, 140–149 (2014)
6. T. Beck, H. Kondziella, G. Huard, T. Bruckner, Assessing the influence of the temporal resolution of electrical load and PV generation profiles on self-consumption and sizing of PV-battery systems. Appl. Energy **173**, 331–342 (2016)
7. Y. Wang, S. Mao, R.M. Nelms, *Online Algorithms for Optimal Energy Distribution in Microgrids* (Springer International Publishing, Berlin, 2015)
8. T. Kato, Y. Manabe, T. Funabashi, K. Yoshiura, M. Kurimoto, Y. Suzuoki, A study on several hours ahead forecasting of spatial average irradiance using NWP model and satellite infrared image, 2016 International Conference on Probabilistic Methods Applied to Power Systems (PMAPS), pp. 1–8 (2016)
9. J.M. Bright, S. Killinger, D. Lingfors, N.A. Engerer, Improved satellite-derived PV power nowcasting using real-time power data from reference PV systems. Sol. Energy **168**, 118–139 (2018)
10. C. David, R. Walter, G.-D. Benjamín, E.S. Les, L. Ricardo Guerrero, First results of a low cost all-sky imager for cloud tracking and intra-hour irradiance forecasting serving a pv-based smart grid in La Graciosa Island, in 2017 IEEE 44th Photovoltaic Specialist Conference (PVSC), pp. 1–5 (2017)
11. A. Shakya, S. Michael, C. Saunders, D. Armstrong, P. Pandey, S. Chalise, R. Tonkoski, Solar irradiance forecasting in remote microgrids using markov switching model. IEEE Trans. Sustain. Energy **8**(3), 895–905 (2017)

12. M.W. Ahmad, M. Mourshed, Y. Rezgui, Tree-based ensemble methods for predicting PV power generation and their comparison with support vector regression. Energy **164**, 465–474 (2018)
13. H. Bouzgou, C.A. Gueymard, Fast short-term global solar irradiance forecasting with wrapper mutual information. Renew. Energy **133**, 1055–1065 (2019)
14. W. El-Baz, P. Tzscheutschler, U. Wagner, Day-ahead probabilistic PV generation forecast for buildings energy management systems. Sol. Energy **171**, 478–490 (2018)
15. H. Verbois, A. Rusydi, A. Thiery, Probabilistic forecasting of day-ahead solar irradiance using quantile gradient boosting. Sol. Energy **173**, 313–327 (2018)
16. P. Mathiesen, J.M. Brown, J. Kleissl, Geostrophic wind dependent probabilistic irradiance forecasts for coastal California. IEEE Trans. Sustain. Energy **4**(2), 510–518 (2013)
17. J.A. Duffie, W.A. Beckman, *Solar Engineering of Thermal Processes*, 4th edn. (John Wiley & Sons, Hoboken, NJ, 2013)
18. Météo-France. https://donneespubliques.meteofrance.fr